

Article

# Performance of Universal Reciprocating Heat-Engine Cycle with Variable Specific Heats Ratio of Working Fluid

Lingen Chen <sup>1,2,\*</sup> , Yanlin Ge <sup>1,2</sup>, Chang Liu <sup>1,2</sup>, Huijun Feng <sup>1,2</sup> and Giulio Lorenzini <sup>3</sup>

<sup>1</sup> Institute of Thermal Science and Power Engineering, Wuhan Institute of Technology, Wuhan 430205, China; geyali9@hotmail.com (Y.G.); lc198707181@126.com (C.L.); huijunfeng@139.com (H.F.)

<sup>2</sup> School of Mechanical & Electrical Engineering, Wuhan Institute of Technology, Wuhan 430205, China

<sup>3</sup> Dipartimento di Ingegneria e Architettura, Università di Parma, Parco Area delle Scienze 181/A, 43124 Parma, Italy; giulio.lorenzini@unipr.it

\* Correspondence: lingenchen@hotmail.com

Received: 6 March 2020; Accepted: 29 March 2020; Published: 31 March 2020



**Abstract:** Considering the finite time characteristic, heat transfer loss, friction loss and internal irreversibility loss, an air standard reciprocating heat-engine cycle model is founded by using finite time thermodynamics. The cycle model, which consists of two endothermic processes, two exothermic processes and two adiabatic processes, is well generalized. The performance parameters, including the power output and efficiency (PAE), are obtained. The PAE versus compression ratio relations are obtained by numerical computation. The impacts of variable specific heats ratio (SHR) of working fluid (WF) on universal cycle performances are analyzed and various special cycles are also discussed. The results include the PAE performance characteristics of various special cycles (including Miller, Dual, Atkinson, Brayton, Diesel and Otto cycles) when the SHR of WF is constant and variable (including the SHR varied with linear function (LF) and nonlinear function (NLF) of WF temperature). The maximum power outputs and the corresponding optimal compression ratios, as well as the maximum efficiencies and the corresponding optimal compression ratios for various special cycles with three SHR models are compared.

**Keywords:** finite time thermodynamics; reciprocating heat-engine cycle; universal cycle; variable specific heat ratio; power output; thermal efficiency

## 1. Introduction

Using finite time thermodynamics (FTT) [1–16] to optimize the performances of practical cycles and processes, a series of achievements were made, including Novikov heat engines [17–21], Curzon–Ahlborn heat engines [22–24], solar-driven engines [25,26], Maisotaenko cycle [27–29], OTEC systems [30–32], Kalina cycle [33], thermoelectric devices [34–39], dissipative heat engine [40], refrigeration cycle [41], earth [42], quantum systems [43–50], economic systems [51,52], chemical systems [53–61], reciprocating internal combustion engines [62–66], etc. In the early studies, for the reciprocating heat-engine cycle (RHEC), the specific heats (SH) of working fluid (WF) were usually assumed to be constant. For the practical cycle, the properties and composition of the WF will change with the occurrence of the combustion reaction. So the SH of WF will also change with the occurrence of the combustion reaction, and this change has a great influence on cycle performance. The variation of SH of WF would inevitably cause variation of the performance, so the studies on air standard (AS) RHEC performance analysis and optimization can be divided into three classes according to the SH of WF models, including the constant SH model, variable SH model and variable SHR model, see the book [64] and review article [65] in detail.

In the first class, Klein [67] studied the net power versus efficiency relations of endoreversible Diesel and Otto cycles, and obtained the maximum work output and the corresponding compression ratio (CR). References [68,69] derived the power output and efficiency (PAE) and performance characteristics (PC) of Diesel [68] and Otto [69] cycles with heat transfer loss (HTL). Angulo-Brown et al. [70] modeled the Otto cycle with friction loss (FL), and studied the impact of FL on the cycle performance. Using expansion and compression efficiencies to define the internal irreversibility loss (IIL), Chen et al. [71] studied the irreversible Otto cycle performance. Qin et al. [72] modeled a universal RHEC (including Otto, Diesel, Brayton, and Atkinson cycles) which was consisted of an endothermic process, an exothermic process and two adiabatic processes, and derived the PAE relation with FL and HTL. Reference [73] founded a more universal RHEC (including Miller, Dual, Atkinson, Brayton, Diesel and Otto cycles) which consisted of two endothermic processes, two exothermic processes and two adiabatic processes, derived the PAE and PC, and gave out the maximum power output and the maximum efficiency orders of each special cycle.

In the second class, Ghatak and Chakraborty [74] studied the impact of variable SH of WF with the LF of temperature on the PAE and PC of endoreversible Dual cycle. Considering the variable SH with the LF of temperature, references [75,76] studied the performances of Dual [75] and Miller [76] cycles with FL and HTL. References [77–80] analyzed the performances of irreversible Otto [77], Atkinson [78], Diesel [79] and Brayton [80] cycles with HTL, IIL and the variable SH of WF with the LF of temperature. Chen et al. [81] established a universal cycle which consisted of two endothermic processes, two exothermic processes and two adiabatic processes with HTL, FL and variable SH of WF and compared the differences of each special cycle performance when the SH of WF were constant and variable. Abu-Nada et al. [82–85] introduced a cycle model with variable SH of WF with the nonlinear function (NLF) of temperature in the performance studies of internal combustion engine cycle. Using the variable SH model introduced in references [82–85], references [86–89] studied the performances of Otto [86], Diesel [87], Atkinson [88] and Dual [89] cycles and analyzed the impacts of loss items on cycle PC.

In the third class, considering the variable SHR of WF with the LF of temperature, Ebrahimi established endoreversible [90] and irreversible [91] Dual cycle, endoreversible Atkinson cycle [92], endoreversible Diesel cycle [93] and irreversible Otto cycle [94] models, and analyzed the impacts of variable SHR and loss items on cycle PC. Moreover, considering the variable SHR of WF with NLF of temperature, references [95–98] proposed the endoreversible Diesel cycle [95], irreversible Atkinson cycle [96], endoreversible [97] and irreversible [98] Dual cycle models, and studied the effects of variable SHR and loss items on cycle PC.

Establishing the universal model and obtaining the universal laws and results are the aims of FTT pursuit, and they are the same for a performance study of RHEC cycle. For the generalized irreversible RHEC model established in references [73,81], there is no work in the open literature which has studied the effect of variable SHR of WF with NLF of temperature on RHEC PC. This paper will combine the generalized irreversible RHEC model established in [73,81] and the variable SHR model of WF with NLF of temperature in [95–98], analyze the outcome and compare the effects of various SHR models on cycle PC. The maximum power outputs (MPOs) and the corresponding optimal compression ratios, as well as the maximum efficiencies and the corresponding optimal compression ratios for various special cycles with three SHR models will be also compared.

## 2. Cycle Model

An AS RHEC model is shown in Figure 1 which contains two adiabatic branches; two endothermic processes with SH of  $C_{in1}$  and  $C_{in2}$ ; and two exothermic processes with SH of  $C_{out1}$  and  $C_{out2}$ , respectively.

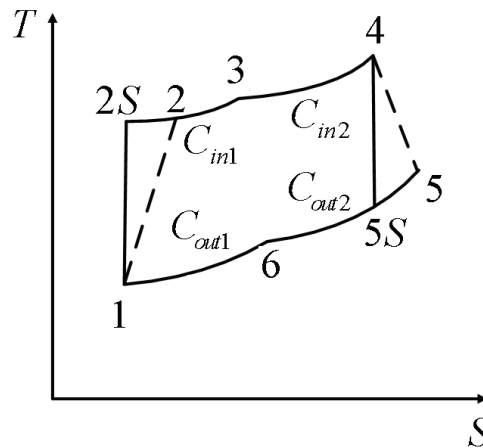


**Figure 1.** The  $T-s$  diagram for an irreversible reciprocating heat-engine cycle (RHEC) model.

When the above four SH are different values, this universal cycle model will be simplified to all kinds of special cycle models. The two irreversible adiabatic processes are shown as  $1 \rightarrow 2$  and  $4 \rightarrow 5$ ; the two heating processes are shown as  $2 \rightarrow 3$  and  $3 \rightarrow 4$ ; and the two cooling processes are shown as  $5 \rightarrow 6$  and  $6 \rightarrow 1$ .

Assuming the SHR of WF varied with temperature with NLF, the SHR  $\gamma$  can be written as

$$\gamma = c + bT + aT^2 \tag{1}$$

where  $a$ ,  $b$  and  $c$  are constants and  $T$  is WF temperature.

It can be supposed that the four thermal capacities of the cycle are

$$\begin{aligned} C_{in1} &= R \frac{m_{in1}(aT^2 + bT) + n_{in1}}{aT^2 + bT + c - 1} & C_{in2} &= R \frac{m_{in2}(aT^2 + bT) + n_{in2}}{aT^2 + bT + c - 1} \\ C_{out1} &= R \frac{m_{out1}(aT^2 + bT) + n_{out1}}{aT^2 + bT + c - 1} & C_{out2} &= R \frac{m_{out2}(aT^2 + bT) + n_{out2}}{aT^2 + bT + c - 1} \end{aligned} \tag{2}$$

where  $m_{in1}$ ,  $m_{in2}$ ,  $m_{out1}$ ,  $m_{out2}$ ,  $n_{in1}$ ,  $n_{in2}$ ,  $n_{out1}$  and  $n_{out2}$  are constants. When  $m_{in1}$  is 1,  $n_{in1}$  is  $c$ , and when  $m_{in1}$  is 0,  $n_{in1}$  is 1, so do  $m_{in2}$  and  $n_{in2}$ ,  $m_{out1}$  and  $n_{out1}$  and  $m_{out2}$  and  $n_{out2}$ .

When the constants have different values, the four thermal capacities can change into the SH with constant pressure and constant volume

$$C_P = \frac{R(aT^2 + bT + c)}{aT^2 + bT + c - 1}, \quad C_V = \frac{R}{aT^2 + bT + c - 1} \tag{3}$$

It can be supposed that two adiabatic processes are instantaneous, and the temperature of WF changes at a constant speed.  $k_1, k_2, k_3$  and  $k_4$  are constants, then the time spent on each cycle is

$$\begin{aligned} \tau &= t_{out2} + t_{out1} + t_{in2} + t_{in1} \\ &= k_4(T_6 - T_1) + k_3(T_5 - T_6) + k_2(T_4 - T_3) + k_1(T_3 - T_2) \end{aligned} \tag{4}$$

The heat addition in the processes  $2 \rightarrow 3$  and  $3 \rightarrow 4$  can be written as

$$\begin{aligned} Q_{in} &= M \left( \int_{T_2}^{T_3} C_{in1} dT + \int_{T_3}^{T_4} C_{in2} dT \right) \\ &= MR \left\{ \begin{aligned} & m_{in1}(T_3 - T_2) + m_{in2}(T_4 - T_3) + [2D^{-1}(m_{in1} - cm_{in1} + n_{in1})] \{ \arctan[D^{-1}(b + 2aT_3)] - \arctan[D^{-1}(b + 2aT_2)] \} \\ & - \{ \arctan[D^{-1}(b + 2aT_3)] - \arctan[D^{-1}(b + 2aT_4)] \} \times [2D^{-1}(m_{in2} - cm_{in2} + n_{in2})] \end{aligned} \right\} \end{aligned} \tag{5}$$

The heat rejection in the processes 5 → 6 and 6 → 1 can be written as

$$Q_{out} = M \left( \int_{T_1}^{T_6} C_{out1} dT + \int_{T_6}^{T_5} C_{out2} dT \right) = MR \left\{ \frac{m_{out1}(T_6 - T_1) + m_{out2}(T_5 - T_6) + [2D^{-1}(m_{out1} - cm_{out1} + n_{out1})] \{ \arctan[D^{-1}(b + 2aT_6)] - \arctan[D^{-1}(b + 2aT_1)] \}}{(b + 2aT_1)} - \{ \arctan[D^{-1}(b + 2aT_6)] - \arctan[D^{-1}(b + 2aT_5)] \} \times [(2D^{-1}(m_{out2} - cm_{out2} + n_{out2}))]} \right\} \quad (6)$$

where  $D = \sqrt{4ac - 4a - b^2}$ ,  $R$  is gas constant and  $M$  is mole number of WF.

The following parameters are defined as

$$r = V_1/V_2, \rho = V_4/V_3, r_p = T_3/T_2, r_c = T_6/T_1 \quad (7)$$

For the two irreversible adiabatic processes, the IIL are defined as the expansion and compression efficiencies [86–89]

$$\eta_C = (T_1 - T_{2S}) / (T_1 - T_2) \quad (8)$$

$$\eta_E = (T_5 - T_4) / (T_{5S} - T_4) \quad (9)$$

According to references [75–81], the expression for reversible adiabatic process when SHR is varied is

$$V^{\gamma-1}T = (V + dV)^{\gamma-1}(T + dT) \quad (10)$$

From Equation (10), one has

$$\frac{1}{c-1} \left\{ \frac{1}{2} \ln \left( \frac{aT_j^2 + bT_j + c-1}{aT_i^2 + bT_i + c-1} \right) + \frac{b}{D} \left\{ \arctan[(2aT_j + b)/D] - \arctan[(2aT_i + b)/D] \right\} - \ln \left( \frac{T_j}{T_i} \right) \right\} = \ln \left( \frac{V_j}{V_i} \right) \quad (11)$$

For the endoreversible adiabatic process 1 → 2S, one has

$$\frac{1}{c-1} \left\{ \frac{1}{2} \ln \left( \frac{aT_{2S}^2 + bT_{2S} + c-1}{aT_1^2 + bT_1 + c-1} \right) + \frac{b}{D} \left\{ \arctan[(2aT_{2S} + b)/D] - \arctan[(2aT_1 + b)/D] \right\} - \ln \left( \frac{T_{2S}}{T_1} \right) \right\} = \ln \left( \frac{1}{r} \right) \quad (12)$$

The special cycles  $m_{in1}$ ,  $m_{in2}$ ,  $m_{out1}$ ,  $m_{out2}$ ,  $n_{in1}$ ,  $n_{in2}$ ,  $n_{out1}$  and  $n_{out2}$  are fixed, and Equation (12) becomes the expression of the adiabatic process for the various special cycles.

After a cycle, the entropy change of the WF is zero, so one has

$$\left\{ \begin{aligned} & m_{in1} \ln(T_3/T_{2S}) + m_{in2} \ln(T_4/T_3) + m_{out1} \ln(T_1/T_6) + m_{out2} \ln(T_6/T_{5S}) + \{ \{ m_{in1}(c-1) - n_{in1} \} [2(c-1)]^{-1} \{ D^{-1}2b \{ -\arctan[D^{-1}(b + 2aT_{2S})] + \arctan[D^{-1}(b + 2aT_3)] \} \} - 2 \\ & \times \ln(T_3/T_{2S}) + \ln[(aT_3^2 + bT_3 + c-1)/(aT_{2S}^2 + bT_{2S} + c-1)] \} + \{ \{ m_{in2}(c-1) - n_{in2} \} [2(1-c)]^{-1} \{ D^{-1}2b \{ -\arctan[D^{-1}(b + 2aT_3)] + \arctan[D^{-1}(b + 2aT_4)] \} \} - 2 \\ & \times \ln(T_4/T_3) + \ln[(aT_4^2 + bT_4 + c-1)/(aT_3^2 + bT_3 + c-1)] \} - \{ \{ m_{out1}(c-1) - n_{out1} \} [2(1-c)]^{-1} \{ D^{-1}2b \{ -\arctan[D^{-1}(b + 2aT_6)] + \arctan[D^{-1}(b + 2aT_1)] \} \} - 2 \\ & \times \ln(T_1/T_6) + \ln[(aT_1^2 + bT_1 + c-1)/(aT_6^2 + bT_6 + c-1)] \} - \{ \{ m_{out2}(c-1) - n_{out2} \} [2(1-c)]^{-1} \{ D^{-1}2b \{ -\arctan[D^{-1}(b + 2aT_{5S})] + \arctan[D^{-1}(b + 2aT_6)] \} \} - 2 \\ & \times \ln(T_6/T_{5S}) + \ln[(aT_6^2 + bT_6 + c-1)/(aT_{5S}^2 + bT_{5S} + c-1)] \} \end{aligned} \right\} = 0 \quad (13)$$

For a practical cycle, there exists HTL and FL. According reference [67], the heat addition rate to the WF by combustion is:

$$Q_{in} = A' - B'[0.5(T_4 + T_2) - T_0] = A - B(T_4 + T_2) \quad (14)$$

where  $A'$  is the heat released by fuel,  $B'$  is heat leakage coefficient,  $T_0$  is the ambient temperature and  $A = A' + B'T_0$  and  $B = B'/2$  are two constants.

According to reference [70], the lost power due to FL is

$$P_\mu = \mu(dX/dt)^2 = \mu\bar{v}^2 \tag{15}$$

The mean velocity of piston motion is

$$\bar{v} = x(r - 1) / \Delta t_{12} \tag{16}$$

where  $\mu$  is the friction coefficient in exhaust stroke,  $\bar{v}$  is the mean velocity of piston,  $X$  is the piston displacement,  $x$  is the piston position at upper dead point and  $\Delta t_{12}$  is the time of the power stroke.

### 3. Power Output and Thermal Efficiency

The net power output is

$$P = (Q_{in} - Q_{out}) / \tau - P_\mu$$

$$MR \left\{ \begin{aligned} & m_{in1}(T_3 - T_2) + m_{in2}(T_4 - T_3) - m_{out1}(T_6 - T_1) - m_{out2}(T_5 - T_6) + [2D^{-1}(m_{in1} - cm_{in1} \\ & + n_{in1})\{\arctan[D^{-1}(b + 2aT_3)] - \arctan[D^{-1}(b + 2aT_2)]\}] + [2D^{-1}(m_{in2} - cm_{in2} \\ & + n_{in2})\{\arctan[D^{-1}(b + 2aT_4)] - \arctan[D^{-1}(b + 2aT_3)]\}] - [2(m_{out1} - cm_{out1} + \\ & n_{out1})/D]\{\arctan[D^{-1}(b + 2aT_6)] - \arctan[D^{-1}(b + 2aT_1)]\}] + [2D^{-1}(m_{out2} - cm_{out2} \\ & + n_{out2})\{\arctan[D^{-1}(b + 2aT_6)] - \arctan[D^{-1}(b + 2aT_5)]\}] \end{aligned} \right\} \tag{17}$$

$$= \frac{\hspace{10em}}{K_4(T_6 - T_1) + K_3(T_5 - T_6) + K_2(T_4 - T_3) + K_1(T_3 - T_2)} - b_f(r - 1)^2$$

where  $b_f$  is defined as  $b_f = \mu x_2^2 / (\Delta t_{12})^2$ .

The thermal efficiency is

$$\eta = P\tau / Q_{in}$$

$$MR \left\{ \begin{aligned} & m_{in1}(T_3 - T_2) + m_{in2}(T_4 - T_3) - m_{out1}(T_6 - T_1) - m_{out2}(T_5 - T_6) - [2D^{-1}(m_{in1} - cm_{in1} + n_{in1})] \\ & \left\{ \arctan[D^{-1}(b + 2aT_2)] - \arctan[D^{-1}(b + 2aT_3)] \right\} - [2D^{-1}(m_{in2} - cm_{in2} + n_{in2})] \\ & \left\{ \arctan[D^{-1}(b + 2aT_3)] - \arctan[D^{-1}(b + 2aT_4)] \right\} + [2D^{-1}(m_{out1} - cm_{out1} + n_{out1})] \\ & \left\{ \arctan[D^{-1}(b + 2aT_1)] - \arctan[D^{-1}(b + 2aT_6)] \right\} + [2D^{-1}(m_{out2} - cm_{out2} + n_{out2})] \\ & \left\{ \arctan[D^{-1}(b + 2aT_6)] - \arctan[D^{-1}(b + 2aT_5)] \right\} \end{aligned} \right\} \tag{18}$$

$$= \frac{-b_f(r - 1)^2 [K_4(T_6 - T_1) + K_3(T_5 - T_6) + K_2(T_4 - T_3) + K_1(T_3 - T_2)]}{MR \left\{ \begin{aligned} & m_{in1}(T_3 - T_2) + m_{in2}(T_4 - T_3) - [2D^{-1}(m_{in1} - cm_{in1} + n_{in1})] \left\{ \arctan[D^{-1}(b + 2aT_2)] - \right. \\ & \left. \arctan[D^{-1}(b + 2aT_3)] \right\} - [2D^{-1}(m_{in2} - cm_{in2} + n_{in2})] \left\{ \arctan[D^{-1}(b + 2aT_3)] - \right. \\ & \left. \arctan[D^{-1}(b + 2aT_4)] \right\} \end{aligned} \right\}}$$

In order to make the cycle run normally, State 3 must be between States 2 and 4. When States 2 and 3 coincide, it gives  $r_p = (r_p)_{min} = 1$ , and when States 3 and 4 coincide, it gives  $r_p = (r_p)_{max}$  and  $T_3 = (r_p)_{max} T_2 = T_4$ .  $T_2$  can be gotten by Equations (12) and (8). Substituting  $T_3 = (r_p)_{max} T_2 = T_4$  into Equations (5) and (14) gives  $(r_p)_{max}$ . So the range of  $r_p$  is

$$1 = (r_p)_{min} \leq r_p \leq (r_p)_{max} \tag{19}$$

State 6 must be between States 1 and 5. When States 1 and 6 coincide, it gives  $r_c = (r_c)_{min} = 1$ , and when States 3 and 4 coincide, it gives  $r_c = (r_c)_{max}$  and  $T_6 = (r_c)_{max} T_1 = T_5$ . Substituting  $T_2$  into Equation (7) gives  $T_3$ , substituting  $T_3$  into Equations (5) and (14) gives  $T_4$  and substituting  $T_6 = (r_c)_{max} T_1 = T_5$  and the temperatures above into Equation (13) gives  $(r_p)_{max}$ . So the range of  $r_c$  is

$$1 = (r_c)_{min} \leq r_c \leq (r_c)_{max} \tag{20}$$

### 4. Discussions

Equations (17) and (18) are the PAE characteristics of the universal cycle which include all kinds of RHEC with different loss items.

(1) When  $m_{in1} = m_{in2} = m_{out1} = m_{out2} = 0$  and  $n_{in1} = n_{in2} = n_{out1} = n_{out2} = 1$ , the expressions can be simplified into the PAE for an AS Otto cycle.

(2) When  $m_{in1} = m_{in2} = 1, n_{in1} = n_{in2} = c, m_{out1} = m_{out2} = 0$  and  $n_{out1} = n_{out2} = 1$ , the expressions can be simplified into the PAE for an AS Diesel cycle.

(3) When  $m_{in1} = m_{in2} = 0, n_{in1} = n_{in2} = 1, m_{out1} = m_{out2} = 1$  and  $n_{out1} = n_{out2} = c$ , the expressions can be simplified into the PAE for an AS Atkinson cycle.

(4) When  $m_{in1} = m_{in2} = m_{out1} = m_{out2} = 1$  and  $n_{in1} = n_{in2} = n_{out1} = n_{out2} = c$ , the expressions can be simplified into the PAE for an AS Brayton cycle.

(5) When  $m_{in1} = 0, m_{in2} = m_{out1} = m_{out2} = n_{in1} = 1$  and  $n_{in2} = n_{out1} = n_{out2} = c$ , the expressions can be simplified into the PAE for an AS Dual cycle.

(6) When  $m_{in1} = m_{in2} = m_{out2} = 0, m_{out1} = n_{in1} = n_{in2} = n_{out2} = 1$  and  $n_{out1} = c$ , the expressions can be simplified into the PAE for an AS Miller cycle.

(7) When  $a \neq 0$ , the expressions can be simplified into the PAE for the universal cycle with variable SHR of WF with the NLF of temperature; when  $a = 0$  and  $b \neq 0$ , the expressions can be turned into those with variable SHR with the LF of temperature; and when  $a = b = 0$ , the expressions can be simplified into those for the constant SHR.

(8) When  $\eta_c \neq 1$  and  $\eta_e \neq 1$ , the expressions can be simplified into the PAE for the universal cycle with IIL, and when  $\eta_c = \eta_e = 1$ , the expressions can be simplified into that for the cycle without IIL.

(9) When  $b_f \neq 0$ , the expressions can be simplified into the PAE for the cycle with FL, and when  $b_f = 0$ , the expressions can be simplified into those for the cycle without FFL.

(10) When  $B \neq 0$ , the expressions can be simplified into the PAE for the cycle with HTL, and when  $B = 0$ , the expressions can be simplified into those for the cycle without HTL.

## 5. Numerical Examples

According to references [81,95–98], the following constants are used in the computations:  $A = 60000 \text{ J/mol}$ ,  $B = 25 \text{ J/(mol} \cdot \text{K)}$ ,  $T_1 = 300 \text{ K}$ ,  $b = -9.7617 \times 10^{-5} \text{ K}^{-1}$ ,  $a = 1.6928 \times 10^{-8} \text{ K}^{-1}$ ,  $c = 1.4235$ ,  $M = 0.0157 \text{ mol}$ ,  $R = 8.314$ ,  $\gamma_p = 1.2$ ,  $\gamma_c = 1.2$ ,  $b_f = 32.5 \text{ W}$ ,  $K_3 = K_4 = 18.67 \times 10^{-6} \text{ s} \cdot \text{K}^{-1}$  and  $K_1 = K_2 = 8.128 \times 10^{-6} \text{ s} \cdot \text{K}^{-1}$ .

Figures 2 and 3 illustrate the relations of power output versus CR and efficiency versus CR for various special cycles with the constant SHR and variable SHR with LF and NLF of temperature. Figure 2 shows that, compared with the constant SHR, the ranges of the CRs of various special cycles with the variable SHR with the LF of temperature increase from 13.5 to about 16, the power output decreases (0.5% decrease for Miller cycle; 3% decrease for Otto and Atkinson cycles; 8% decrease for Diesel, Brayton and Dual cycles). Compared with the variable SHR with the LF of temperature, the ranges of CR of various special cycles with the variable SHR with NLF of temperature decrease from 16 to about 15; the changes of power output are unobvious (0.5% increase for Diesel cycle; 0.1% increase for Dual cycle; about 0.5–2% decrease for Otto, Atkinson, Brayton and Miller cycles). The order of the maximum power outputs (MPO) of various special cycles is  $P_{br} > P_{at} > P_{mi} > P_{du} > P_{di} > P_{ot}$  with every one of the three SHR models.

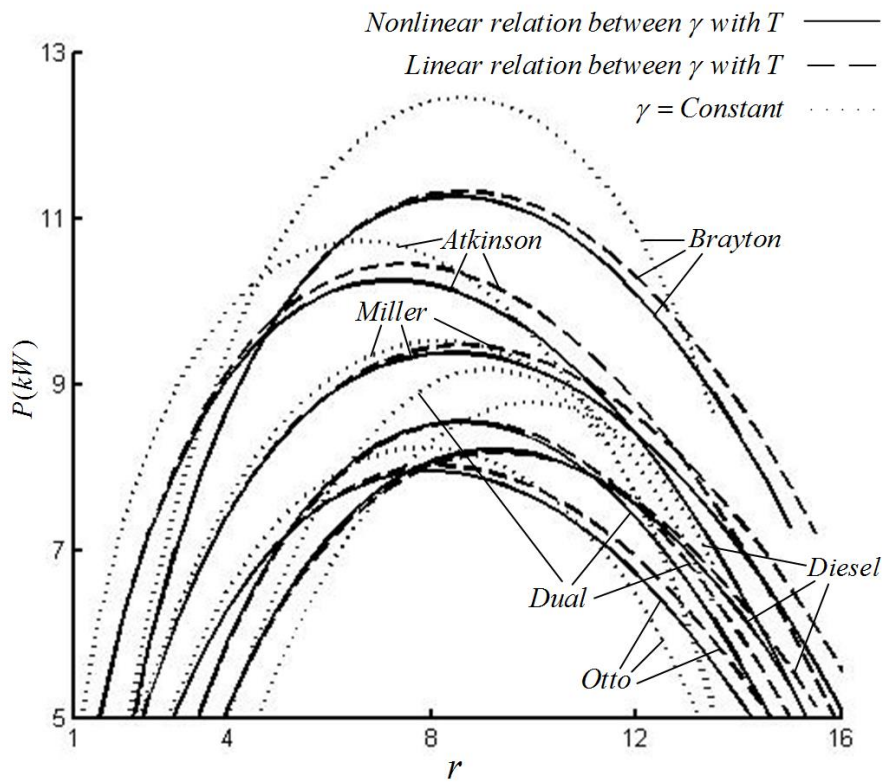


Figure 2. The power output versus CR for various special cycles.

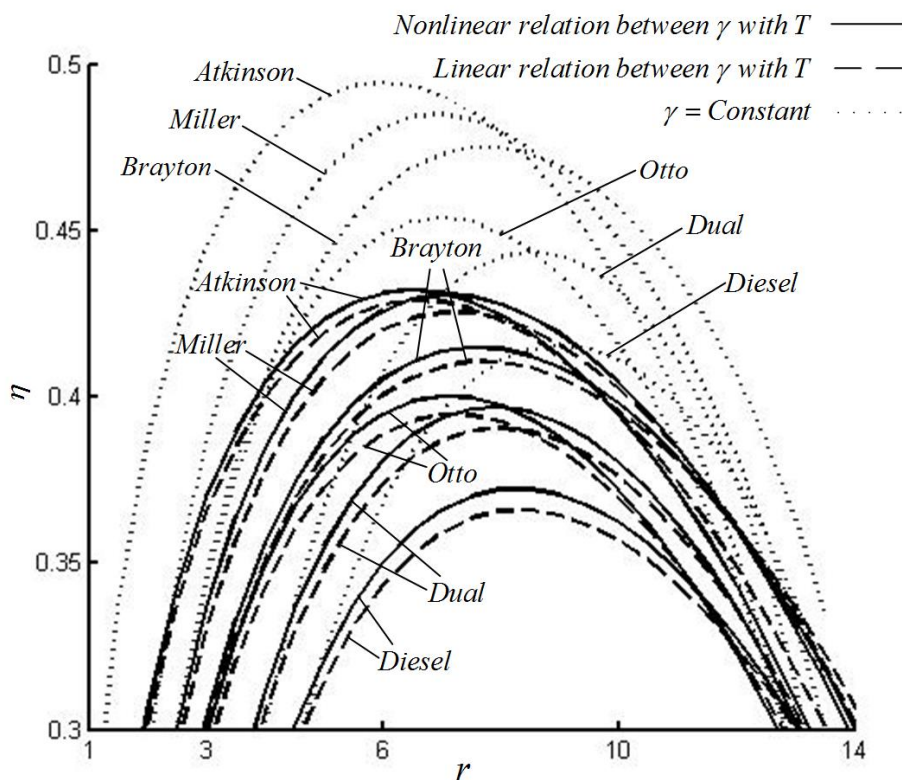


Figure 3. The efficiency versus compression ratio (CR) for various special cycles.

For the Otto cycle, under three SHR models, the orders of the MPOs and the corresponding optimal CRs are  $(P_{ot})_C > (P_{ot})_L > (P_{ot})_N$  and  $(r_{ot})_L > (r_{ot})_N > (r_{ot})_C$ . For the Diesel cycle, under three SHR models, the orders of the MPOs and the corresponding optimal CRs are  $(P_{di})_C > (P_{di})_N > (P_{di})_L$

and  $(r_{di})_C > (r_{di})_L > (r_{di})_N$ . For Atkinson cycle, under three SHR models, the orders of the MPOs and the corresponding optimal CRs are  $(P_{at})_C > (P_{at})_L > (P_{at})_N$  and  $(r_{at})_L > (r_{at})_N > (r_{at})_C$ . For the Brayton cycle, under three SHR models, the orders of the MPOs and the corresponding optimal CRs are  $(P_{br})_C > (P_{br})_L > (P_{br})_N$  and  $(r_{br})_L > (r_{br})_C > (r_{br})_N$ . For the Dual cycle, under three SHR models, the orders of the MPOs and the corresponding optimal CRs are  $(P_{du})_C > (P_{du})_L > (P_{du})_N$  and  $(r_{du})_C > (r_{du})_L > (r_{du})_N$ . For the Miller cycle, under three SHR models, the orders of the MPOs and the corresponding optimal CRs are  $(P_{mi})_C > (P_{mi})_L > (P_{mi})_N$  and  $(r_{mi})_L > (r_{mi})_N > (r_{mi})_C$ . Under constant SHR model, the order of the corresponding optimal CRs at the MPO points of various special cycles is  $r_{di} > r_{du} > r_{br} > r_{mi} > r_{ot} > r_{at}$ . Under variable SHR with the LF of the temperature model, the order of the corresponding optimal CRs at the MPO points of various special cycles is  $r_{di} > r_{br} > r_{mi} > r_{du} > r_{ot} > r_{at}$ . Under variable SHR with NLF of temperature model, the order of the corresponding optimal CRs at the MPO points of various special cycles is  $r_{di} > r_{du} > r_{mi} > r_{br} > r_{ot} > r_{at}$ .

Figure 3 shows that, compared with the constant SHR, the efficiencies of various special cycles with the variable SHR with the LF of temperature decrease by about 12%. Compared with the variable SHR with the LF of temperature, the efficiencies of various special cycles with variable SHR with NLF of temperature increase by about 0.7–1.7%. The order of the maximum efficiency of various special cycles is  $\eta_{at} > \eta_{mi} > \eta_{br} > \eta_{ot} > \eta_{du} > \eta_{di}$  with every one of the three SHR models.

For the Otto cycle, under three SHR models, the orders of the maximum efficiencies and corresponding optimal CRs are  $(\eta_{ot})_C > (\eta_{ot})_N > (\eta_{ot})_L$  and  $(r_{ot})_C > (r_{ot})_L > (r_{ot})_N$ . For the Diesel cycle, under three SHR models, the orders of the maximum efficiencies and corresponding optimal CRs are  $(\eta_{di})_C > (\eta_{di})_N > (\eta_{di})_L$  and  $(r_{di})_C > (r_{di})_N > (r_{di})_L$ . For the Atkinson cycle, under three SHR models, the orders of the maximum efficiencies and corresponding optimal CRs are  $(\eta_{at})_C > (\eta_{at})_N > (\eta_{at})_L$  and  $(r_{at})_L > (r_{at})_N > (r_{at})_C$ . For the Brayton cycle, under three SHR models, the orders of the maximum efficiencies and corresponding optimal CRs are  $(\eta_{br})_C > (\eta_{br})_N > (\eta_{br})_L$  and  $(r_{br})_C > (r_{br})_N > (r_{br})_L$ . For the Dual cycle, under three SHR models, the orders of the maximum efficiencies and corresponding optimal CRs are  $(\eta_{du})_C > (\eta_{du})_N > (\eta_{du})_L$  and  $(r_{du})_C > (r_{du})_N > (r_{du})_L$ . For the Miller cycle, under three SHR models, the orders of the maximum efficiencies and corresponding optimal CRs are  $(\eta_{mi})_C > (\eta_{mi})_N > (\eta_{mi})_L$  and  $(r_{mi})_L > (r_{mi})_N > (r_{mi})_C$ .

Under the constant SHR model, the order of the corresponding optimal CRs at the maximum efficiency points of various special cycles is  $r_{di} > r_{du} > r_{br} > r_{ot} > r_{mi} > r_{at}$ . Under variable SHR with the LF of temperature model, the order of the corresponding optimal CRs at the maximum efficiency points of various special cycles is  $r_{di} > r_{du} > r_{br} > r_{mi} > r_{ot} > r_{at}$ . Under variable SHR with NLF of temperature model, the order of the corresponding optimal CRs at the maximum efficiency points of various special cycles is  $r_{di} > r_{du} > r_{br} > r_{ot} > r_{mi} > r_{at}$ .

In general, the optimal CR at MPO point is not the same as the optimal CR at maximum efficiency point, for all discussed cycles with three SHR models. The reasonable design range for all of the discussed cycles with three SHR models should be between the optimal CR at MPO point and the optimal CR at maximum efficiency point from the point of view of compromised optimization of the PAE.

From what was mentioned above, one can see that there are influences of the variable SHR model on the performance of every special cycle; and the performances of Miller, Brayton and Atkinson cycles are more excellent than those of Otto, Diesel and Dual cycles with every one of the three SHR models.

## 6. Conclusions

The AS RHEC model considering HTL, FL and IIL is established in this paper. The cycle performances with various SHR are analyzed. The performance parameters including the PAE are derived. The performances of all kinds of special cycles are discussed and the MPO and the maximum efficiency of each special cycle and the corresponding optimal CRs are compared. The results show that the orders of the MPO and the maximum efficiency remain the same with every one of the three SHR models, but the PAE changes, which suggests that the various SHRs have influences on cycle

performance. When the model of variable SHR is more complicated, the distance between the cycle model and the practice one is closer. The reasonable design range for various cycles should be between the optimal CR at MPO point and the optimal CR at maximum efficiency point for the compromise optimization of the PAE.

**Author Contributions:** L.C., Y.G., C.L., H.F. and G.L. equally contributed to the manuscript. All authors have read and agreed to the published version of the manuscript.

**Acknowledgments:** This paper is supported by the National Natural Science Foundation of China (project number 51779262). The author wishes to thank four reviewers for their careful, unbiased and constructive suggestions, which led to this revised manuscript.

**Conflicts of Interest:** The authors declare no conflict of interest.

## Nomenclature

<i>A</i>	heat rate released by fuel
<i>B</i>	constant related to heat transfer
<i>C</i>	specific heat
<i>M</i>	mole number of WF
<i>P</i>	power output
<i>Q</i>	heat added or rejected by the working fluid
<i>r</i>	compression ratio
<i>T</i>	temperature
<i>V</i>	volume
Greek symbol	
$\gamma$	SHR
$\eta$	efficiency
$\eta_c$	compression efficiency
$\eta_E$	expansion efficiency
Subscripts	
<i>at</i>	Atkinson cycle
<i>br</i>	Brayton cycle
<i>C</i>	Constant SHR
<i>di</i>	Diesel cycle
<i>du</i>	Dual cycle
<i>L</i>	Variable SHR with the LF of temperature
<i>mi</i>	Miller cycle
<i>N</i>	Variable SHR with NLF of temperature
<i>ot</i>	Otto cycle

## Abbreviations

AS	air standard
CR	compression ratio
FL	friction loss
FTT	finite time thermodynamics
HTL	heat transfer loss
IIL	internal irreversibility loss
LF	linear function
MPO	maximum power output
NLF	nonlinear function
PAE	power output and efficiency
PC	performance characteristics
RHEC	reciprocating heat-engine cycle
SH	specific heat
SHR	specific heat ratio
WF	working fluid

## References

1. Andresen, B. *Finite-Time Thermodynamics*; University of Copenhagen Physics Laboratory II: Copenhagen, Denmark, 1983.
2. Hoffmann, K.H.; Burzler, J.M.; Schubert, S. Endoreversible thermodynamics. *J. Non Equilib. Thermodyn.* **1997**, *22*, 311–355.
3. Chen, L.G.; Wu, C.; Sun, F.R. Finite time thermodynamic optimization or entropy generation minimization of energy systems. *J. Non Equilib. Thermodyn.* **1999**, *24*, 327–359. [[CrossRef](#)]
4. Hoffman, K.H.; Burzler, J.; Fischer, A.; Schaller, M.; Schubert, S. Optimal process paths for endoreversible systems. *J. Non Equilib. Thermodyn.* **2003**, *28*, 233–268. [[CrossRef](#)]
5. Andresen, B. Current trends in finite-time thermodynamics. *Angew. Chem. Int. Ed.* **2011**, *50*, 2690–2704. [[CrossRef](#)] [[PubMed](#)]
6. Feidt, M. Optimum thermodynamics-New upperbounds. *Entropy* **2009**, *11*, 529–547. [[CrossRef](#)]
7. Vaudrey, A.V.; Lanzetta, F.; Feidt, M.H.B. Reitlinger and the origins of the efficiency at maximum power formula for heat engines. *J. Non Equilib. Thermodyn.* **2014**, *39*, 199–204. [[CrossRef](#)]
8. Feidt, M. The history and perspectives of efficiency at maximum power of the Carnot engine. *Entropy* **2017**, *19*, 369. [[CrossRef](#)]
9. Feidt, M. *Finite Physical Dimensions Optimal Thermodynamics 1. Fundamental*; ISTE Press: London, UK; Elsevier: London, UK, 2017.
10. Feidt, M. *Finite Physical Dimensions Optimal Thermodynamics 2. Complex Systems*; ISTE Press: London, UK; Elsevier: London, UK, 2018.
11. Chen, L.G.; Xia, S.J. *Generalized Thermodynamic Dynamic-Optimization for Irreversible Processes*; Science Press: Beijing, China, 2017.
12. Chen, L.G.; Xia, S.J. *Generalized Thermodynamic Dynamic-Optimization for Irreversible Cycles—Thermodynamic and Chemical Theoretical Cycles*; Science Press: Beijing, China, 2018.
13. Chen, L.G.; Xia, S.J. *Generalized Thermodynamic Dynamic-Optimization for Irreversible Cycles –Engineering Thermodynamic Plants and Generalized Engine Cycles*; Science Press: Beijing, China, 2018.
14. Chen, L.G.; Xia, S.J. Progresses in generalized thermodynamic dynamic-optimization of irreversible processes. *Sci. Sin. Technol.* **2019**, *49*, 981–1022. [[CrossRef](#)]
15. Chen, L.G.; Xia, S.J.; Feng, H.J. Progress in generalized thermodynamic dynamic-optimization of irreversible cycles. *Sci. Sin. Technol.* **2019**, *49*, 1223–1267. [[CrossRef](#)]
16. Chen, L.G.; Li, J. *Thermodynamic Optimization Theory for Two-Heat-Reservoir Cycles*; Science Press: Beijing, China, 2020.
17. Schwalbe, K.; Hoffmann, K.H. Performance features of a stationary stochastic Novikov engine. *Entropy* **2018**, *20*, 52. [[CrossRef](#)]
18. Schwalbe, K.; Hoffmann, K.H. Stochastic Novikov engine with time dependent temperature fluctuations. *Appl. Therm. Eng.* **2018**, *142*, 483–488. [[CrossRef](#)]
19. Schwalbe, K.; Hoffmann, K.H. Novikov engine with fluctuating heat bath temperature. *J. Non Equilib. Thermodyn.* **2018**, *43*, 141–150. [[CrossRef](#)]
20. Schwalbe, K.; Hoffmann, K.H. Stochastic Novikov engine with Fourier heat transport. *J. Non Equilib. Thermodyn.* **2019**, *44*, 417–424. [[CrossRef](#)]
21. Feidt, M.; Costea, M. Progress in Carnot and Chambadal modeling of thermomechanical engine by considering entropy and heat transfer entropy. *Entropy* **2019**, *21*, 1232. [[CrossRef](#)]
22. Feidt, M.; Costea, M.; Petrescu, S.; Stanciu, C. Nonlinear thermodynamic analysis and optimization of a Carnot engine cycle. *Entropy* **2016**, *18*, 243. [[CrossRef](#)]
23. Páez-Hernández, R.T.; Chimal-Eguía, J.C.; Ladino-Luna, D.; Velázquez-Arcos, J.M. Comparative performance analysis of a simplified Curzon-Ahlborn engine. *Entropy* **2018**, *20*, 637. [[CrossRef](#)]
24. Gonzalez-Ayala, J.; Santillán, M.; Santos, M.J.; Calvo-Hernández, A.; Roco, J.M.M. Optimization and stability of heat engines: The role of entropy evolution. *Entropy* **2018**, *20*, 865. [[CrossRef](#)]
25. Barranco-Jimenez, M.A.; Sanchez-Salas, N.; Angulo-Brown, F. Finite time thermoeconomic optimization of a solar-driven heat engine model. *Entropy* **2011**, *13*, 171–183. [[CrossRef](#)]
26. Schwalbe, K.; Hoffmann, K.H. Optimal control of an endoreversible solar power plant. *J. Non Equilib. Thermodyn.* **2018**, *43*, 255–271. [[CrossRef](#)]

27. Zhu, F.L.; Chen, L.G.; Wang, W.H. Thermodynamic analysis of an irreversible Maisotsenko reciprocating Brayton cycle. *Entropy* **2018**, *20*, 167. [[CrossRef](#)]
28. Zhu, F.L.; Chen, L.G.; Wang, W.H. Thermodynamic analysis and optimization of irreversible Maisotsenko-Diesel cycle. *J. Therm. Sci.* **2019**, *28*, 659–668. [[CrossRef](#)]
29. Shen, J.F.; Chen, L.G.; Ge, Y.L.; Zhu, F.L.; Wu, Z.X. Optimum ecological performance of irreversible reciprocating Maisotsenko-Brayton cycle. *Euro. Phys. J. Plus* **2019**, *134*, 293. [[CrossRef](#)]
30. Fontaine, K.; Yasunaga, T.; Ikegami, Y. OTEC maximum net power output using Carnot cycle and application to simplify heat exchanger selection. *Entropy* **2019**, *21*, 1143. [[CrossRef](#)]
31. Yasunaga, T.; Ikegami, Y. Finite-time thermodynamic model for evaluating heat engines in ocean thermal energy conversion. *Entropy* **2020**, *22*, 211. [[CrossRef](#)]
32. Wu, Z.X.; Feng, H.J.; Chen, L.G.; Tang, W.; Shi, J.Z.; Ge, Y.L. Constructal thermodynamic optimization for ocean thermal energy conversion system with dual-pressure organic Rankine cycle. *Energy Convers. Manag.* **2020**, *210*, 112727. [[CrossRef](#)]
33. Feng, H.J.; Qin, W.X.; Chen, L.G.; Cai, C.G.; Ge, Y.L.; Xia, S.J. Power output, thermal efficiency and exergy-based ecological performance optimizations of an irreversible KCS-34 coupled to variable temperature heat reservoirs. *Energy Convers. Manag.* **2020**, *205*, 112424. [[CrossRef](#)]
34. Chen, L.G.; Meng, F.K.; Sun, F.R. Thermodynamic analyses and optimizations for thermoelectric devices: The state of the arts. *Sci. China Technol. Sci.* **2016**, *59*, 442–455. [[CrossRef](#)]
35. Feng, Y.L.; Chen, L.G.; Meng, F.K.; Sun, F.R. Influences of Thomson effect on performance of thermoelectric generator-driven thermoelectric heat pump combined device. *Entropy* **2018**, *20*, 29. [[CrossRef](#)]
36. Feng, Y.L.; Chen, L.G.; Meng, F.K.; Sun, F.R. Influences of external heat transfer and Thomson effect on performance of TEG-TEC combined thermoelectric device. *Sci. China Technol. Sci.* **2018**, *61*, 1600–1610. [[CrossRef](#)]
37. Feng, Y.L.; Chen, L.G.; Meng, F.K.; Sun, F.R. Thermodynamic analysis of TEG-TEC device including influence of Thomson effect. *J. Non Equilib. Thermodyn.* **2018**, *43*, 75–86. [[CrossRef](#)]
38. Pourkiaei, S.M.; Ahmadi, M.H.; Sadeghzadeh, M.; Moosavi, S.; Pourfayaz, F.; Chen, L.G.; Yazdi, M.A.; Kumar, R. Thermoelectric cooler and thermoelectric generator devices: A review of present and potential applications, modeling and materials. *Energy* **2019**, *186*, 115849. [[CrossRef](#)]
39. Chen, L.G.; Meng, F.K.; Ge, Y.L.; Feng, H.J.; Xia, S.J. Performance optimization of a class of combined thermoelectric heating devices. *Sci. China Technol. Sci.* **2020**, *63*. [[CrossRef](#)]
40. Masser, R.; Hoffmann, K.H. Dissipative endoreversible engine with given efficiency. *Entropy* **2019**, *21*, 1117. [[CrossRef](#)]
41. Stanciu, C.; Feidt, M.; Costea, M.; Stanciu, D. Optimization and entropy production: Application to Carnot-like refrigeration machines. *Entropy* **2018**, *20*, 953. [[CrossRef](#)]
42. Arango-Reyes, K.; Barranco-Jiménez, M.A.; De Parga-Álvarez, G.A.; Angulo-Brown, F. A simple thermodynamic model of the internal convective zone of the earth. *Entropy* **2018**, *20*, 985. [[CrossRef](#)]
43. Kosloff, R. Quantum thermodynamics: A dynamical viewpoint. *Entropy* **2013**, *15*, 2100–2128. [[CrossRef](#)]
44. Hoffmann, K.H.; Salamon, P. Finite-time availability in a quantum system. *EPL* **2015**, *109*, 40004. [[CrossRef](#)]
45. Kosloff, R.; Rezek, Y. The quantum harmonic Otto cycle. *Entropy* **2017**, *19*, 136. [[CrossRef](#)]
46. Deffner, S. Efficiency of harmonic quantum Otto engines at maximal power. *Entropy* **2018**, *20*, 875. [[CrossRef](#)]
47. Chen, L.G.; Liu, X.W.; Wu, F.; Xia, S.J.; Feng, H.J. Exergy-based ecological optimization of an irreversible quantum Carnot heat pump with harmonic oscillators. *Phys. A Stat. Mech. Appl.* **2020**, *537*, 122597. [[CrossRef](#)]
48. Liu, X.W.; Chen, L.G.; Wei, S.H.; Meng, F.K. Optimal ecological performance investigation of a quantum harmonic oscillator Brayton refrigerator. *Trans. ASME J. Therm. Sci. Eng. Appl.* **2020**, *12*, 1–24. [[CrossRef](#)]
49. Yin, Y.; Chen, L.G.; Wu, F.; Ge, Y.L. Work output and thermal efficiency of an endoreversible entangled quantum Stirling engine with a 1D isotropic Heisenberg model. *Phys. A Stat. Mech. Appl.* **2020**. [[CrossRef](#)]
50. Chen, L.G.; Liu, X.W.; Wu, F.; Feng, H.J.; Xia, S.J. Power and efficiency optimization of an irreversible quantum Carnot heat engine working with harmonic oscillators. *Phys. A Stat. Mech. Appl.* **2020**. [[CrossRef](#)]
51. Chen, Y. Maximum profit configuration of commercial engines. *Entropy* **2011**, *13*, 1137–1151. [[CrossRef](#)]
52. Sieniutycz, S. *Complexity and Complex Thermo-Economic Systems*; Elsevier: Oxford, UK, 2020.
53. Zhang, L.; Chen, L.G.; Xia, S.J.; Wang, C.; Sun, F.R. Entropy generation minimization for reverse water gas shift (RWGS) reactor. *Entropy* **2018**, *20*, 415. [[CrossRef](#)]

54. Roach, T.N.F.; Salamon, P.; Nulton, J.; Andresen, B.; Felts, B.; Haas, A.; Calhoun, S.; Robinett, N.; Rohwer, F. Application of finite-time and control thermodynamics to biological processes at multiple scales. *J. Non Equilib. Thermodyn.* **2018**, *43*, 193–210. [\[CrossRef\]](#)
55. Chen, L.G.; Zhang, L.; Xia, S.J.; Sun, F.R. Entropy generation minimization for hydrogenation of CO<sub>2</sub> to light olefins. *Energy* **2018**, *147*, 187–196. [\[CrossRef\]](#)
56. Chen, L.G.; Wang, C.; Xia, S.J.; Sun, F.R. Thermodynamic analysis and optimization of extraction process of CO<sub>2</sub> from acid seawater by using hollow fiber membrane contactor. *Int. J. Heat Mass Transf.* **2018**, *124*, 1310–1320. [\[CrossRef\]](#)
57. Chimal-Eguia, J.C.; Paez-Hernandez, R.; Ladino-Luna, D.; Velázquez-Arcos, J.M. Performance of a simple energetic-converting reaction model using linear irreversible thermodynamics. *Entropy* **2019**, *21*, 1030. [\[CrossRef\]](#)
58. Li, P.L.; Chen, L.G.; Xia, S.J.; Zhang, L. Entropy generation rate minimization for in methanol synthesis via CO<sub>2</sub> hydrogenation reactor. *Entropy* **2019**, *21*, 174. [\[CrossRef\]](#)
59. Zhang, L.; Xia, S.J.; Chen, L.G.; Ge, Y.L.; Wang, C.; Feng, H.J. Entropy generation rate minimization for hydrocarbon synthesis reactor from carbon dioxide and hydrogen. *Int. J. Heat Mass Transf.* **2019**, *137*, 1112–1123. [\[CrossRef\]](#)
60. Zhang, L.; Chen, L.G.; Xia, S.J.; Ge, Y.L.; Wang, C.; Feng, H.J. Multi-objective optimization for helium-heated reverse water gas shift reactor by using NSGA-II. *Int. J. Heat Mass Transf.* **2020**, *148*, 119025. [\[CrossRef\]](#)
61. Li, P.L.; Chen, L.G.; Xia, S.J.; Zhang, L.; Kong, R.; Ge, Y.L.; Feng, H.J. Entropy generation rate minimization for steam methane reforming reactor heated by molten salt. *Energy Rep.* **2020**, *6*, 685–697. [\[CrossRef\]](#)
62. Zhao, J.X.; Xu, F.C. Finite-time thermodynamic modeling and a comparative performance analysis for irreversible Otto, Miller and Atkinson Cycles. *Entropy* **2018**, *20*, 75. [\[CrossRef\]](#)
63. Wu, Z.X.; Chen, L.G.; Feng, H.J. Thermodynamic optimization for an endoreversible Dual-Miller cycle (DMC) with finite speed of piston. *Entropy* **2018**, *20*, 165. [\[CrossRef\]](#)
64. Medina, A.; Curto-Risso, P.L.; Calvo-Hernández, A.; Guzmán-Vargas, L.; Angulo-Brown, F.; Sen, A.K. *Quasi-Dimensional Simulation of Spark Ignition Engines. From Thermodynamic Optimization to Cyclic Variability*; Springer: London, UK, 2014.
65. Ge, Y.L.; Chen, L.G.; Sun, F.R. Progress in finite time thermodynamic studies for internal combustion engine cycles. *Entropy* **2016**, *18*, 139. [\[CrossRef\]](#)
66. Ge, Y.L.; Chen, L.G.; Qin, X.Y. Effect of specific heat variations on irreversible Otto cycle performance. *Int. J. Heat Mass Transf.* **2018**, *122*, 403–409. [\[CrossRef\]](#)
67. Klein, S.A. An explanation for observed compression ratios in international combustion engines. *Trans. ASME J. Eng. Gas Turbine Power* **1991**, *113*, 511–513. [\[CrossRef\]](#)
68. Chen, L.G.; Wu, C.; Sun, F.R. Heat transfer effects on the net work output and efficiency characteristics for an air standard Otto cycle. *Energy Convers. Manag.* **1998**, *39*, 643–648. [\[CrossRef\]](#)
69. Chen, L.G.; Zen, F.M.; Sun, F.R.; Wu, C. Heat transfer effects on the net work output and power as function of efficiency for air standard Diesel cycle. *Energy* **1996**, *21*, 1201–1205. [\[CrossRef\]](#)
70. Angulo-Brown, F.; Fernandez-Betanzos, J.; Diaz-Pico, C.A. Compression ratio of an optimized Otto-cycle model. *Eur. J. Phys.* **1994**, *15*, 38–42. [\[CrossRef\]](#)
71. Rocha-Martinez, J.A.; Navarrete-Gonzalez, T.D.; Pava-Miller, C.G.; Ramirez-Rojas, A.; Angulo-Brown, F. Otto and Diesel engine models with cyclic variability. *Rev. Mex. Fis.* **2002**, *48*, 228–234.
72. Qin, X.Y.; Chen, L.G.; Sun, F.R. The universal power and efficiency characteristics for irreversible reciprocating heat engine cycles. *Eur. J. Phys.* **2003**, *24*, 359–366. [\[CrossRef\]](#)
73. Ge, Y.L.; Chen, L.G.; Sun, F.R.; Wu, C. Reciprocating heat-engine cycles. *Appl. Energy* **2005**, *81*, 180–186. [\[CrossRef\]](#)
74. Ghatak, A.; Chakraborty, S. Effect of external irreversibilities and variable thermal properties of working fluid on thermal performance of a Dual ICE cycle. *Stroj. Casopsis (J. Mech. Energy)* **2007**, *58*, 1–12.
75. Chen, L.G.; Ge, Y.L.; Sun, F.R.; Wu, C. Effects of heat transfer, friction and variable specific heats of working fluid on performance of an irreversible Dual cycle. *Energy Convers. Manag.* **2006**, *47*, 3224–3234. [\[CrossRef\]](#)
76. Chen, L.G.; Ge, Y.L.; Sun, F.R.; Wu, C. The performance of a Miller cycle with heat transfer, friction and variable specific heats of working fluid. *Termotecnica* **2010**, *14*, 24–32.
77. Ge, Y.L.; Chen, L.G.; Sun, F.R.; Wu, C. The effects of variable specific heats of working fluid on the performance of an irreversible Otto cycle. *Int. J. Exergy* **2005**, *2*, 274–283. [\[CrossRef\]](#)

78. Ge, Y.L.; Chen, L.G.; Sun, F.R.; Wu, C. Performance of Atkinson cycle with heat transfer, friction and variable specific heats of working fluid. *Appl. Energy* **2006**, *83*, 1210–1221. [[CrossRef](#)]
79. Ge, Y.L.; Chen, L.G.; Sun, F.R.; Wu, C. Performance of Diesel cycle with heat transfer, friction and variable specific heats of working fluid. *J. Energy Inst.* **2007**, *80*, 239–242. [[CrossRef](#)]
80. Ge, Y.L.; Chen, L.G.; Sun, F.R.; Wu, C. Performance of reciprocating Brayton cycle with heat transfer, friction and variable specific heats of working fluid. *Int. J. Ambient. Energy* **2008**, *29*, 65–75. [[CrossRef](#)]
81. Chen, L.G.; Ge, Y.L.; Sun, F.R. Unified thermodynamic description and optimization for a class of irreversible reciprocating heat engine cycles. *Proc. IMechE Part D J. Automob. Eng.* **2008**, *222*, 1489–1500. [[CrossRef](#)]
82. Abu-Nada, E.; Al-Hinti, I.; Al-Aarkhi, A.; Akash, B. Thermodynamic modeling of spark-ignition engine: Effect of temperature dependent specific heats. *Int. Commun. Heat Mass Transf.* **2005**, *33*, 1264–1272. [[CrossRef](#)]
83. Abu-Nada, E.; Al-Hinti, I.; Al-Aarkhi, A.; Akash, B. Thermodynamic analysis of spark-ignition engine using a gas mixture model for the working fluid. *Int. J. Energy Res.* **2007**, *37*, 1031–1046. [[CrossRef](#)]
84. Abu-Nada, E.; Al-Hinti, I.; Al-Aarkhi, A.; Akash, B. Effect of piston friction on the performance of SI engine: A new thermodynamic approach. *ASME Trans. J. Eng. Gas Turbine Power* **2008**, *130*, 022802. [[CrossRef](#)]
85. Abu-Nada, E.; Akash, B.; Al-Hinti, I.; Al-Sarkhi, A. Performance of spark-ignition engine under the effect of friction using gas mixture model. *J. Energy Inst.* **2009**, *82*, 197–205. [[CrossRef](#)]
86. Ge, Y.L.; Chen, L.G.; Sun, F.R. Finite time thermodynamic modeling and analysis for an irreversible Otto cycle. *Appl. Energy* **2008**, *85*, 618–624. [[CrossRef](#)]
87. Ge, Y.L.; Chen, L.G.; Sun, F.R. Finite time thermodynamic modeling and analysis for an irreversible Diesel cycle. *Proc. IMechE Part D J. Automob. Eng.* **2008**, *222*, 887–894. [[CrossRef](#)]
88. Ge, Y.L.; Chen, L.G.; Sun, F.R. Finite time thermodynamic modeling and analysis for an irreversible Atkinson cycle. *Therm. Sci.* **2010**, *14*, 887–896. [[CrossRef](#)]
89. Ge, Y.L.; Chen, L.G.; Sun, F.R. Finite time thermodynamic modeling and analysis for an irreversible Dual cycle. *Comput. Math. Model.* **2009**, *50*, 101–108. [[CrossRef](#)]
90. Ebrahimi, R. Thermodynamic simulation of performance of an endoreversible Dual cycle with variable specific heat ratio of working fluid. *J. Am. Sci.* **2009**, *5*, 175–180.
91. Ebrahimi, R. Effects of cut-off ratio on performance of an irreversible Dual cycle. *J. Am. Sci.* **2009**, *5*, 83–90.
92. Ebrahimi, R. Performance of an endoreversible Atkinson cycle with variable specific heat ratio of working fluid. *J. Am. Sci.* **2010**, *6*, 12–17.
93. Ebrahimi, R. Effects of variable specific heat ratio of working fluid on performance of an endoreversible Diesel cycle. *J. Energy Inst.* **2010**, *83*, 1–5. [[CrossRef](#)]
94. Ebrahimi, R. Thermodynamic modeling of an irreversible dual cycle: Effect of mean piston speed. *Rep. Opin.* **2009**, *1*, 25–30.
95. Ebrahimi, R. Performance of an irreversible Diesel cycle under variable stroke length and compression ratio. *J. Am. Sci.* **2009**, *5*, 58–64.
96. Ebrahimi, R. Effects of mean piston speed, equivalence ratio and cylinder wall temperature on performance of an Atkinson engine. *Math. Comput. Model.* **2011**, *53*, 1289–1297. [[CrossRef](#)]
97. Ebrahimi, R. Effects of pressure ratio on the network output and efficiency characteristics for an endoreversible Dual cycle. *J. Energy Inst.* **2011**, *84*, 30–33. [[CrossRef](#)]
98. Ebrahimi, R. Performance analysis of a dual cycle engine with considerations of pressure ratio and cut-off ratio. *Acta Phys. Polon. A* **2010**, *118*, 534–539. [[CrossRef](#)]

